Mem. S.A.It. Vol. 82, 800

Memorie della

Particle acceleration at supernova shocks in young stellar clusters

A.M. Bykov[1], P.E. Gladilin[1], and S.M. Osipov[1,2]

[1] A.F.Ioffe Physical-Technical Institute, St. Petersburg, Russia
e-mail: byk@astro.ioffe.ru
[2] State Politechnical University, St. Petersburg, Russia

Abstract. We briefly discuss models of energetic particle acceleration by supernova shock in active starforming regions at different stages of their evolution. Strong shocks may strongly amplify magnetic fields due to cosmic ray driven instabilities. We discuss the magnetic field amplification emphasizing the role of the long-wavelength instabilities. Supernova shock propagating in the vicinity of a powerful stellar wind in a young stellar cluster is argued to increase the maximal CR energies at a given evolution stage of supernova remnant (SNR) and can convert a sizeable fraction of the kinetic energy release into energetic particles.

1. Introduction

The observed spectra of Galactic cosmic rays (CRs) are shaped by two basic processes - the acceleration in the sources and the subsequent propagation in cosmic magnetic fields and radiation fields. A transition from galactic to extragalactic cosmic rays is expected to occur somewhere between 10^{17} eV and 10^{19} eV (e.g. Hillas, 2005; Aharonian et al., 2011). A preponderance of evidence suggests that the particle acceleration mechanism most likely responsible is diffusive shock acceleration (DSA) (e.g., Blandford & Eichler, 1987; Jones & Ellison, 1991; Malkov & Drury, 2001).

An important question for DSA and CR origin has always centered around the maximum particle energy a given shock can produce. For a shock of a given size, age, and magnetic field geometry, the maximum CR energy depends mainly on the power in the longest wavelength turbulence. The weakly anisotropic distribution of accelerated particles, i.e., CRs is considered in § 2 as an agent producing this turbulence in a symbiotic relationship where the magnetic turbulence required to accelerate the CRs is created by the accelerated CRs themselves.

Other important issue of the high energy CR acceleration models is the environment where the supernova exploded. Some models of CRs acceleration by SNRs in active star forming regions are briefly discussed in § 3. OB-associations and young globular clusters are observed both in the Milky Way and LMC. The study of the stellar content of the galactic object Cygnus OB2 by Knödlseder (2000) have revealed that the number of OB member stars can be estimated as large as 2600 ± 400, while the number of O stars amounts to 120 ± 20. The high number of stellar X-ray sources detected with *Chandra* by Wright &

Send offprint requests to: A.M. Bykov

Drake (2009) confirmed the status of Cygnus OB2 as one of the most massive SFRs in the Milky Way. Given the apparently compact size of Cygnus OB2 one may expect a number of massive stars with strong winds to be in a close proximity with less than 10 pc separation in addition to the well known colliding-wind binaries that are expected to be particle accelerators (e.g. Eichler & Usov, 1993). Another very compact young stellar cluster Westerlund 2 containing more than dozen O stars was found in the Carina region with estimated age to be younger than 4 Myrs, so the most massive stars are expected to explode there within the next few Myrs. OB associations with supernova explosions are creating superbubbles (SBs). Bamba et al. (2004) discovered both thermal and nonthermal X-rays from the shells of the SB 30 Dor C in the LMC. The X-ray morphology was reported as a nearly circular shell with a radius of 40 pc, which is bright on the northern and western sides. Maddox et al. (2009) analyzed *Suzaku* observations of the SB around the OB association LH9 in the HII complex N11 in the Large Magellanic Cloud. Their X-ray spectral analysis revealed that the hard X-ray emission (> 2 keV) requires a hard nonthermal power-law component. The energy budget analysis for N11 using the known stellar content of LH9 indicated that the observed thermal and kinetic energy in the SB is only half of the expected mechanical energy injected by stars, consistent with the expectation of SB models with efficient CR acceleration (e.g. Bykov, 2001; Butt & Bykov, 2008). Diffuse X-ray emission was detected from many sites of massive star formation: the Carina Nebula, M17, 30 Doradus, NGC 3576, NGC 3603, and others (e.g. Townsley et al., 2011). The H.E.S.S. telescope detected high-energy gamma rays from starburst galaxy NGC 253 supporting the ideas of efficient CR acceleration in active starforming regions (Acero, 2009).

2. Magnetic field amplification in CR acceleration sources

Fast and efficient CR acceleration by Fermi mechanism requires that particles are multiply scattered by magnetic fluctuations in the acceleration source (e.g. shock). The magnitude of the required magnetic fluctuations is substantially higher than the ambient magnetic turbulence forcing a bootstrap scenario where the accelerated particles amplify the turbulence required for their acceleration. The study of turbulence generation associated with CRs and DSA has a long history. Magnetic field amplification due to the resonant cosmic-ray streaming instability was studied in the context of galactic cosmic-ray origin and propagation since the 1960s (see e.g. Kulsrud & Cesarsky, 1971; Wentzel, 1974; Achterberg, 1981; Berezinskii et al., 1990; Zweibel, 2003). It was proposed by Bell (1978) as a source of magnetic turbulence in the test particle DSA scenario, and nonlinear models of DSA including CR-driven instabilities and magnetic field amplification were investigated by Bell (2004); Amato & Blasi (2006); Zirakashvili & Ptuskin (2008),Vladimirov et al. (2008, 2009) and Reville et al. (2009).

It is instructive to summarize the growth rates for magnetic instabilities that the quasi-linear theory predicts for weakly anisotropic CR distributions of the form

$$f(\mathbf{p}) = \frac{\mathbf{N}}{\mathbf{4}\pi}\left[\mathbf{1} + \mathbf{3}\beta_{\mathbf{s}}\mu + \frac{\delta}{\mathbf{2}}\left(\mathbf{3}\mu^{\mathbf{2}} - \mathbf{1}\right)\right], \qquad (1)$$

where θ - particle pitch-angle, $\mu = \cos\theta$, $\beta_s = u_s/c$, with the flow (shock) velocity u_s, $\delta(p)$ - is the magnitude of the second harmonic anisotropy. We included here the second harmonic anisotropy to illustrate the effect of the CR-firehose instability on the magnetic field amplification. The substantial anisotropy of the second harmonics can be expected in more complex plasma flows than just an isolated shock. The isotropic part of the distribution function is a power-law of the form

$$N(p) = \frac{n_{cr}\,(\alpha-3)\,p_0^{(\alpha-3)}}{\left[1-\Delta^{\alpha-3}\right]p^{\alpha}}, \qquad (2)$$

where the CR momenta $p_0 \le p \le p_m$, $\Delta = \frac{p_m}{p_0}$, α - is the CR power law index, and n_{cr}- is the CR number density. The CR mean free path $\Lambda = \eta r_g(p)$, where the particle gyroradius is $r_g(p) = \frac{cp}{eB_0}$ and $\eta \ge 1$. Then, following the

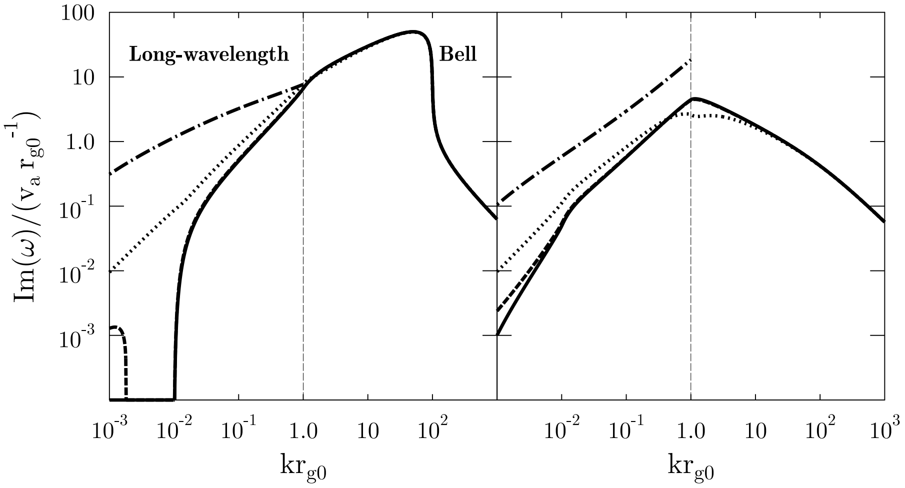

Fig. 1. The two panels show the growth rates for two opposite circular polarization modes (shown in left and right panels) of the parallel propagating modes as a function of the wavenumber. The CR resonant streaming instability and the Bell instability The dot-dashed curves effect of short-scale turbulence on the long-wavelength instability. The model parameters are $\Delta = 100, \beta_s = 0.01$ and $\alpha = 4.0$. For comparison, the dot-dashed curves are calculated for the model of the ponderomotive CR current instability in the presence of the short-scale turbulence (Bykov et al., 2011). The dotted curves illustrate the maximal case of the CR-firehose instability (i.e., $\delta \propto \beta_s$). The dashed curve corresponds to $\delta = 5\beta_s^2$.

standard linear analysis of the kinetic equation *in the intermediate regime* $\eta^{-1} < x_0 < 1$ (see e.g. Bykov et al., 2011) one may get the following dispersion relation:

$$\frac{\omega^2}{v_a^2 k^2} = \left[1 \mp \frac{k_0}{k}\left\{A_0 - 1 + \frac{\delta}{\beta_s}A_1\right\}\right]. \tag{3}$$

$$A_{0,1}(x_0, x_m) = \int_{p_0}^{p_m} \sigma_{0,1}(p)\, N(p)\, p^2 dp \tag{4}$$

$$\sigma_0(p) = \frac{3}{4}\int_{-1}^{1} \frac{\left(1-\mu^2\right)}{1 \mp x\mu} d\mu, \tag{5}$$

$$\sigma_1(p) = \frac{3}{4}\int_{-1}^{1} \frac{\left(1-\mu^2\right)\mu}{1 \mp x\mu} d\mu \tag{6}$$

where $k_0 = \dfrac{4\pi}{c}\dfrac{en_{cr}u_s}{B_0}$, $x = kr_g(p)$, $x_0 = kr_g(p_0)$, $x_m = kr_g(p_m)$. The signs $\pm$ correspond to the two opposite circularly polarized modes under investigation. The second term in the right hand site in corresponds to the fast growing mode discovered by Bell (2004) for $x_0 > 1$. The instability results in amplification of a mode with wavenumbers $k_0 > k > \dfrac{1}{r_{g0}}$. For $x_0 < 1$ the term in Eq. 3 is responsible for the well known resonant streaming instability (e.g. Achterberg, 1981; Zweibel, 2003; Pelletier et al., 2006; Marcowith et al., 2006; Amato & Blasi, 2009, and the references therein). The last term in the r.h.s. of Eq. 3 described the CR firehose instability. In the long-wavelength regime $x_m \ll 1$ a simplified form of Eq. 3 can be derived

$$\frac{\omega^2}{v_a^2 k^2} = 1 \mp \frac{k_0 r_{g0}}{5}\left[x_m \pm \frac{\delta\beta_s^{-1}\ln\Delta}{(1-\Delta^{-1})}\right]. \tag{7}$$

The growth rates of the unstable modes from the dispersion relation Eq. 3 are shown in Figure 1. The growth rates of the resonant and the Bell instabilities are shown by solid lines in Figure 1. Since $x_m \propto k$ at $x_m \sim 1$, the growth rate $Im(\omega) \propto k^{3/2}$ – the long-wavelength regime pointed out by Schure &

Bell (2011) (for $\Delta = 100$). At longer wavelengths however the second term in the square brackets in Eq. (7) dominate and the CR-firehose type instability appear at $x_m << 1$. The CR-firehose instability rate is indicated by the dashed line at the left panel in Figure 1. The CR-firehose instability may even dominate the regime $Im(\omega) \propto k^{3/2}$ in the case of the second harmonic comparable with the first harmonic (CR current) of the anisotropy, i.e. $\delta \propto \beta_s$. The CR-firehose growth rate in that regime is shown by the dotted curve in Figure 1. That likely requires a more complicated structure of the magnetic field in the flow. The flow in the vicinity of the SNR colliding with a powerful stellar wind (see e.g. Velázquez et al., 2003) discussed below as the PeV CR acceleration site may be relevant. To derive the growth rates of the modes in the long-wavelength regime $k\Lambda < 1$ (i.e. $x_0 < \eta^{-1}$) the collisionless kinetic equation approach discussed above is not appropriate. One should average the kinetic equation for the relativistic particles, the equations of the bulk plasma motions and the induction equation over the ensemble of the short scale fluctuations produced by CR instabilities in the collisionless regime e.g. by the fast Bell instability. In the presence of the short-scale fluctuations, the momentum exchange between the CRs and the flow in the hydrodynamic regime, results in a ponderomotive force that depends on the CR current in the mean-field momentum equation of bulk plasma (Bykov et al., 2011). As a result, there exist transverse growing modes with wavevectors along the initial magnetic field with growth rates that are proportional to the turbulent coefficients determined by the short scale fluctuations. The magnetic field amplification in that regime only weakly depends on the shock velocity [as it follows from Eq. (48) in Bykov et al. (2011)], that is important for the evolution of the maximal energy of CRs accelerated by DSA.

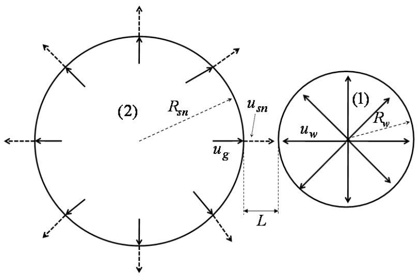

Fig. 2. Simplified view of the expanding supernova remnant approaching a powerful stellar wind. The configuration is shown to be favorable for 10^{15} eV regime CR proton acceleration at a few thousands years old SNR in SFRs. R_w and R_{sn} are the radii of the stellar wind termination shock and SNR forward shock, respectively. u_w is velocity of the stellar wind, u_{sn} is the SNR forward shock velocity, L is the distance between the two flows.

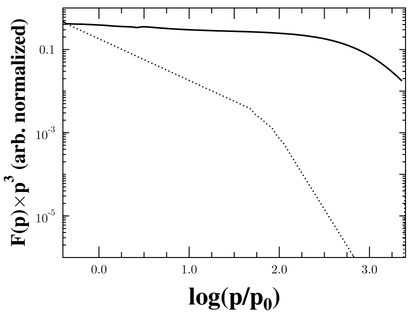

Fig. 3. CR particle spectrum (solid line) from the time-dependent DSA simulation of the SNR forward shock approaching the O-star wind termination shock [see Figure 2]. For the comparison the CR spectrum at solitary shock is shown as the dotted line curve.

3. Particle acceleration by a supernova remnant in OB association

The maximal energies of CRs accelerated by supernova shocks with magnetic field amplification can reach the knee region of the GCR spectrum (e.g. Blandford & Eichler, 1987; Bell, 2004; Berezhko & Völk, 2007; Caprioli et al., 2011). Moreover, it was recently argued by Ptuskin et al. (2010) that the maximum energy of accelerated particles differs strongly for different supernova types. The energy may exceed 10^{17} eV for protons accelerated in an isolated Type IIb SNR. The highest energies CRs are thought to be accelerated before the Sedov stage in isolated SNRs.

For supernova exploded in a young stellar cluster the presence of a nearby strong stellar wind allow to increase the maximum energy of accelerated particles comparing to that in an isolated SNR. The SNRs can produce the high energy CRs at the Sedov evolution stage.

The most massive O stars begin to explode as core collapsed supernovae about a few million years after the formation of a young stellar cluster. The young stars with masses above $\sim 16\,M_\odot$ (of B0 V type and earlier) are thought to create hot low-density bubbles and HII regions with radii ~ 10 pc surrounded by a massive shell of matter swept up from the parent cloud by the stellar wind. In this case, a strong supernova shock propagates for a few thousand years in tenuous circumstellar matter with a velocity well above 10^3 km/s before reaching the dense massive shell. The blast wave of the SNR is expected to accelerate the wind material producing ultra-relativistic ions and electrons. The accelerated particles escape from the SNR forward shock presumably at the highest energy regime (e.g. Ptuskin et al., 2010; Gabici, 2011; Ellison & Bykov, 2011) and can reach the termination shock of the stellar wind of a nearby massive star. We modeled the energetic particle acceleration in the region where the expanding supernova shell is approaching a powerful stellar wind of a young massive star as it is illustrated in Figure 2. At the evolution stage where the mean free path of the highest energy CR is comparable to the distance between the two shocks L the system is characterized by an unusually hard spectral energy distribution illustrated by the solid line in Figure 3. The stage can last more than 1,000 yrs. For comparison we showed with the dotted line the CR spectrum accelerated by an isolated SNR shock of the same age. The case of Bohm diffusion was simulated with $D(p) \propto p$.

A simple analytical kinetic model of particle acceleration by the Fermi mechanism in the converging flows carrying fluctuating magnetic fields amplified by anisotropic CR distributions can be considered. It is a model of high energy CR acceleration by a SNR expanding in a compact OB-association. At some expansion phase the distance L between the SNR approaching the stellar wind shock is less than the mean free path of the highest energy CR particle in the SNR shock precursor. Then CR distribution function around the shocks ($i = 1, 2$) can be approximated as

$$f_i\,(x, p, t) = A p^{-3} \exp\left(-\tfrac{u_i}{D_i}\,|x|\right) \times \\ \times H\,(p - p_0)\,H\,(t - \tau_a) \tag{8}$$

where the highest energy CR acceleration time

$$\tau_a = \int\limits_{p_0}^{p} \frac{3}{(u_1 + u_2)} \left(\frac{D_1}{u_1} + \frac{D_2}{u_2}\right) \frac{dp}{p}. \tag{9}$$

The acceleration mechanism can provide efficient creation of a nonthermal particle population with a very hard energy spectrum, containing a substantial part of the kinetic energy released by the supernova. The high energy nonthermal emission of the sources is characterized by a very hard spectral energy distribution peaked at the maximal photon energies and have the apparent properties of the ”dark accelerators”. The TeV source in the vicinity of the γ-Cygni SNR can be belong to the class.

At the later stage of the young stellar cluster evolution multiple supernova explosions with great energy release in the form of shock waves inside the superbubbles are argued as a favorable site of nonthermal particle acceleration. The collective effect of both stellar winds of massive stars and core collapsed supernovae as particle acceleration agents were discussed by Bykov & Toptygin (2001); Parizot et al. (2004); Torres & Domingo-Santamaría (2007); Ferrand & Marcowith (2010).

Acknowledgements. A.M.B. thanks A.Marcowith for the very interesting CRISM meeting. The authors were supported in part by the Russian government grant 11.G34.31.0001 to Sankt-Petersburg State Politechnical University, and also by the RAS Presidium Program and by the RFBR grant 11-02-12082. They performed the simulations at the Joint Supercomputing Centre (JSCC RAS) and the Supercomputing Centre at Ioffe Institute, St. Petersburg.

References

Acero, F. e. a. 2009, Science, 326, 1080
Achterberg, A. 1981, A&A, 98, 161
Aharonian, F. et al. 2011, Space Sci. Rev., 56
Amato, E., & Blasi, P. 2006, MNRAS, 371, 1251
Amato, E., & Blasi, P. 2009, MNRAS, 392, 1591
Bamba, A. et al. 2004, ApJ, 602, 257
Bell, A. R. 1978, MNRAS, 182, 147
Bell, A. R. 2004, MNRAS, 353, 550
Berezhko, E. G., & Völk, H. J. 2007, ApJ, 661, L175
Berezinskii, V. S. et al. 1990, Astrophysics of cosmic rays (North-Holland, 1990)
Blandford, R., & Eichler, D. 1987, Phys. Rep., 154, 1
Butt, Y. M., & Bykov, A. M. 2008, ApJ, 677, L21
Bykov, A. M. 2001, Space Sci. Rev., 99, 317
Bykov, A. M., Osipov, S. M., & Ellison, D. C. 2011, MNRAS, 410, 39
Bykov, A. M., & Toptygin, I. N. 2001, Astronomy Letters, 27, 625
Caprioli, D., Blasi, P., & Amato, E. 2011, Astroparticle Physics, 34, 447
Eichler, D., & Usov, V. 1993, ApJ, 402, 271
Ellison, D. C., & Bykov, A. M. 2011, ApJ, 731, 87
Ferrand, G., & Marcowith, A. 2010, A&A, 510, A101+
Gabici, S. 2011, this volume, `ArXiv 1108.4844`
Hillas, A. M. 2005, J. Phys. G, 31, R95
Jones, F. C., & Ellison, D. C. 1991, Space Sci. Rev., 58, 259
Knödlseder, J. 2000, A&A, 360, 539
Kulsrud, R. M. 2005, Plasma physics for astrophysics (Princeton University Press)
Kulsrud, R. M., & Cesarsky, C. J. 1971, Astrophys. Lett., 8, 189
Maddox, L. A. et al. 2009, ApJ, 699, 911
Malkov, M. A., & Drury, L. 2001, Reports on Progress in Physics, 64, 429
Marcowith, A., Lemoine, M., & Pelletier, G. 2006, A&A, 453, 193
Parizot, E. et al. 2004, A&A, 424, 747
Pelletier, G., Lemoine, M., & Marcowith, A. 2006, A&A, 453, 181
Ptuskin, V., Zirakashvili, V., & Seo, E. 2010, ApJ, 718, 31
Reville, B., Kirk, J. G., & Duffy, P. 2009, ApJ, 694, 951
Schure, K. M., & Bell, A. R. 2011, MNRAS in press, `ArXiv 1107.5817`
Torres, D. F., & Domingo-Santamaría, E. 2007, Ap&SS, 309, 345
Townsley, L. K. et al. 2011, ApJS, 194, 16
Velázquez, P. F., Koenigsberger, G., & Raga, A. C. 2003, ApJ, 584, 284
Vladimirov, A. E., Bykov, A. M., & Ellison, D. C. 2008, ApJ, 688, 1084
Vladimirov, A. E., Bykov, A. M., & Ellison, D. C. 2009, ApJ, 703, L29
Wentzel, D. G. 1974, Ann. Rev. Astron. Astroph., 12, 71
Wright, N. J., & Drake, J. J. 2009, ApJS, 184, 84
Zirakashvili, V. N., & Ptuskin, V. S. 2008, ApJ, 678, 939
Zweibel, E. G. 2003, ApJ, 587, 625